Modified self-amplifying RNA mediates robust and prolonged gene expression in the mammalian brain

Authors: Jennifer Freire[1,2*], Joshua E. McGee[1*], Dana Shaw[1,3], Yuxin Zhou[1], Yangyang Wang[1], Colin Porter[1,3], Lauren Dang[1,4], Erynne San Antonio[1], Ziqing Yu[1], Kexin Li[1], Wilson W. Wong[1, 5#], Mark W. Grinstaff[1,6#] & Xue Han[1#]

[1]Department of Biomedical Engineering, Boston University, Boston, MA, USA.

[2]Department of Pharmacology, Physiology, and Biophysics, Boston, University, Boston, MA, USA.

[3]Graduate Program for Neuroscience, Boston University, Boston, MA, USA.

[4]Undergraduate Program for Neuroscience, Boston University, Boston, MA, USA.

[5]Biological Design Center, Boston University, Boston, MA, USA.

[6]Department of Chemistry, Boston University, Boston, MA, USA.

[*]These authors contributed equally: Jennifer Freire, Joshua E. McGee.

[#]Correspondence: xuehan@bu.edu, mgrin@bu.edu, wilwong@bu.edu

ABSTRACT

In self-amplifying RNA (saRNA), substitution of cytidine with 5-hydroxymethylcytidine (hm5C) reduces innate immune responses and prolongs protein expression. When formulated as a vaccine and administered intramuscularly, lipid nanoparticles (LNPs) loaded with modified saRNA (saRNA-LNPs) afford robust and long-term protein expression. Here we report the protein expression and cell type tropism of modified saRNA-LNPs, encoding fluorescent proteins, when injected in the mammalian brain. saRNA encapsulated in an LNP formulation comprising ALC-0315 (present in Comirnaty®) efficiently mediates robust and long-lasting protein expression in brain cells beyond five weeks, with detectable expression in some neurons at three months. hm5C saRNA substantially outperforms N1mΨ mRNA. Intriguingly, in addition to transfecting astrocytes and neurons at the injection site, saRNA-LNPs labels neurons retrogradely. Thus, saRNA-LNPs are an exciting nonviral gene transduction method that effectively transduces brain cells with excellent potency and mediates prolonged gene expression.

KEYWORDS

Immune evasion, central nervous system, modified saRNA, gene transfer, astrocytes, neurons

INTRODUCTION

The ability to genetically modify brain cells is advancing our understanding of the brain and offers exciting therapeutic possibilities[1-4]. While viral transduction remains the most effective method for nucleic acid delivery in the central nervous system, it presents significant limitations in payload capacity and safety concerns for clinical applications. Non-viral ribonucleic acid (RNA) technologies offer promising potential to advance the therapeutic development for neurological and psychiatric diseases[1, 5, 6]. Unlike deoxyribonucleic acid (DNA), messenger ribonucleic acid (mRNA) does not require nuclear entry, thereby eliminating the risk of genomic integration associated with DNA-based methods. The development and successful clinical outcomes of mRNA-based COVID vaccines, which incorporated the groundbreaking discovery of chemically modified nucleotides (N1mΨ) to reduce mRNA immunogenicity and enhance translation efficiency, highlight the potential of mRNA therapeutics.[7-10]

Efforts to deliver mRNA encapsulated in lipid nanoparticles (LNPs) to brain cells demonstrate technical feasibility, though with limited transfection efficiency and a short half-life. For example, a landmark study in 2001 by Kariko *et al.* reported that injecting mRNA encapsulated in cationic lipofectin into the rat brain leads to immediate protein expression within 1 hour, but the expression becomes largely undetectable after about 24 hours[11]. More recent attempts in delivering mRNA loaded LNPs to brain cells intracerebrally or intraventricularly highlight improved transfection efficiency[12-16], but nonetheless fail to mediate long lasting gene expression due to the inherent limitation of the short half-life of the mRNA transcripts. Finally, the cargo payload capacity of mRNA limits its utility.

Self-amplifying RNAs (saRNAs) encode an RNA-dependent RNA polymerase and replicate themselves inside the cell, resulting in sustained production of protein encoding RNA while providing a large payload capacity (~10k nucleotides). Intracerebral administration of a heme oxygenase-1 encoding wild-type saRNA, encapsulated in deoxycholic acid-conjugated polyethylenimine, affords persistent protein expression for over 7 days in the brain[17]. However, like mRNA, wild-type saRNAs induce innate immune responses. Past attempts to reduce saRNA immunogenicity, including incorporating N1mΨ modification, failed to preserve transfection potency[18-27]. We recently discovered that complete substitution of cytidine with 5-hydroxymethylcytidine (hm5C) and 5-methylcytidine (m5C) reduces immunogenicity and prolongs protein expression. When encoded for the SARS-CoV spike protein and packaged in LNPs, m5C saRNA is a significantly more potent vaccine than conventional N1mΨ mRNA ones[28]. Motivated by the improved safety profile and transfection efficiency of modified saRNA, we examined the ability of saRNA-LNPs to transfect brain cells when delivered intracerebrally. We selected hm5C as the modification for saRNA, building upon previous studies that showed efficient transcription and translation[28]. We first screened leading LNPs and identified a formulation comprising ALC-0315 (present in Comirnaty, BioNTech/Pfizer) as the most effective LNP, and then systematically evaluated the time course and cell type tropism of saRNA-LNP mediated fluorescent protein expression in the mouse brain.

RESULTS

ALC0315 containing LNPs effectively deliver saRNA to mammalian brain cells

To evaluate the transfection efficiency of saRNA in the brain, we first screened four leading LNP formulations, comprised of an ionizable lipid, DOPE, cholesterol, and DMG-PEG2K at molar ratios of 50:10:38.5:1.5. The ionizable lipids were SM102 (Spikevax®, Moderna), ALC-0315 (Comirnaty®, BioNTech/Pfizer), L319[29] , and Lipid A9. We loaded hm5C modified saRNA encoding either mCherry or GFP into these LNP formulations. The saRNA-LNPs possessed a size between 100-200nm (Fig. 1B), a polydispersity index <0.2 (Fig. 1C), and an encapsulation efficiency >80% (Fig. 1D). We then intracerebrally injected these saRNA-LNPs into the striatum of mice (625 ng, 5μL at 125 ng/μL, Fig. 1E), and quantified protein expression three days post injection by visualizing cellular fluorescence in brain slices. All LNP formulations, except SM102, mediated prominent fluorophore expressions (Fig. 1F-H), with ALC-0315 exhibiting the highest protein expression (Fig. 1F, Hii).

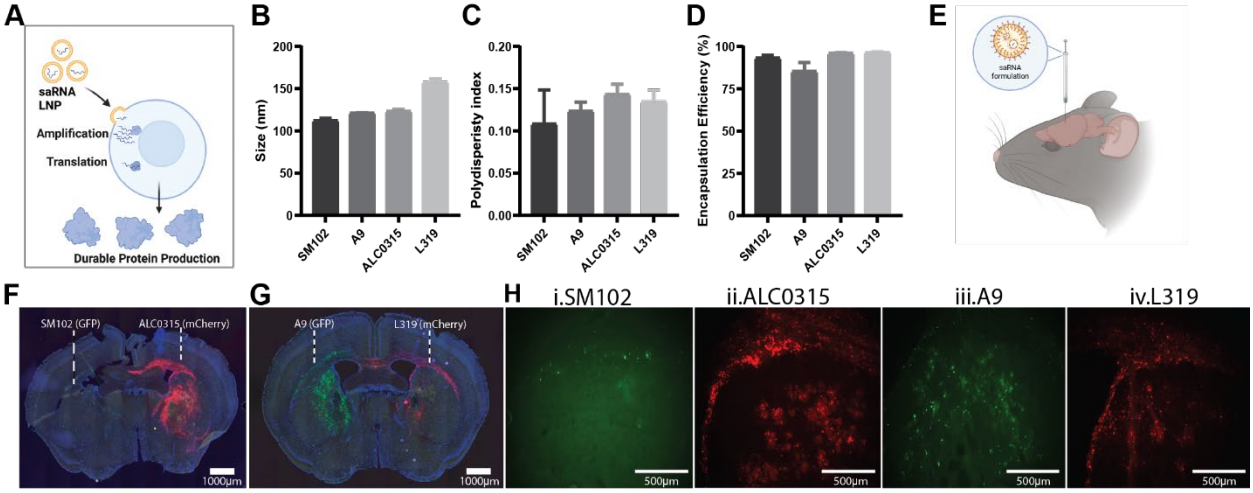

Figure 1. Screen LNPs for efficient saRNA delivery into brain cells. (A) Conceptual illustration of saRNA-LNP mediated protein expression. **(B-D)** Size (B), polydispersity (C), and encapsulation efficiency (D) of LNP formulations comprising SM102, A9, ALC-0315, and L319. **(E)** Illustration of experimental testing in the mouse brain. **(F, G)** Transfection efficiency of the four LNPs loaded with saRNA encoding GFP or mCherry. Shown are GFP (green), mCherry (red) and DAPI (blue) fluorescence at 3 days post saRNA-LNP injection. **(H)** Zoom-in views of F and G showing GFP (green) and mCherry (red) fluorescence.

saRNA-LNPs mediate robust and prolonged gene expression in the brain

To quantify the efficiency and the time course of saRNA-LNP mediated gene expression, we injected the most effective LNP composition comprised of ALC-0315 loaded with saRNA encoding mCherry into the mouse striatum. As a comparison, another cohort of animals received ALC-0315 LNPs loaded with conventional N1mΨ mRNA encoding mCherry (mRNA-LNPs). One day after saRNA-LNP or mRNA-LNP injection, prominent mCherry expression was present around the injection site, which persisted throughout many weeks post injection (Fig. 2A). Surprisingly, mCherry expression was also evident throughout the corpus callosum, suggesting robust labeling of neuronal axons or myelin.

We next estimated the tissue volume transduced by manually segmenting the mCherry-positive area around the striatal injection site and throughout the corpus callosum. mCherry expression progressively increased over the first week, with saRNA-LNP and mRNA-LNPs transfecting similar area in both the striatum and the corpus callosum within the first three days post injection (Fig. 2B, C), but with mRNA-LNPs transfecting a greater area than saRNA-LNPs at one week. However, mRNA-LNP mediated mCherry expression quickly declined after one week, dropping to nearly undetectable levels in most mice by week four. In contrast, saRNA-LNP mediated expression remained prominent until week five at the injection site and in the corpus callosum. In one animal examined at three months post saRNA-LNP injection, the longest time-point evaluated, robust mCherry fluorescence was present in some neurons, throughout both the soma and neuronal processes (Supp. Fig. 1). The persistent saRNA-mediated transcript expression in neurons, though sparse, even at three months after a single injection further underscore the effectiveness of saRNA mediated neuronal transfection. Together, these results demonstrate that chemically modified saRNA mediates more robust and prolonged gene expression in brain cells than conventional N1mΨ mRNAs.

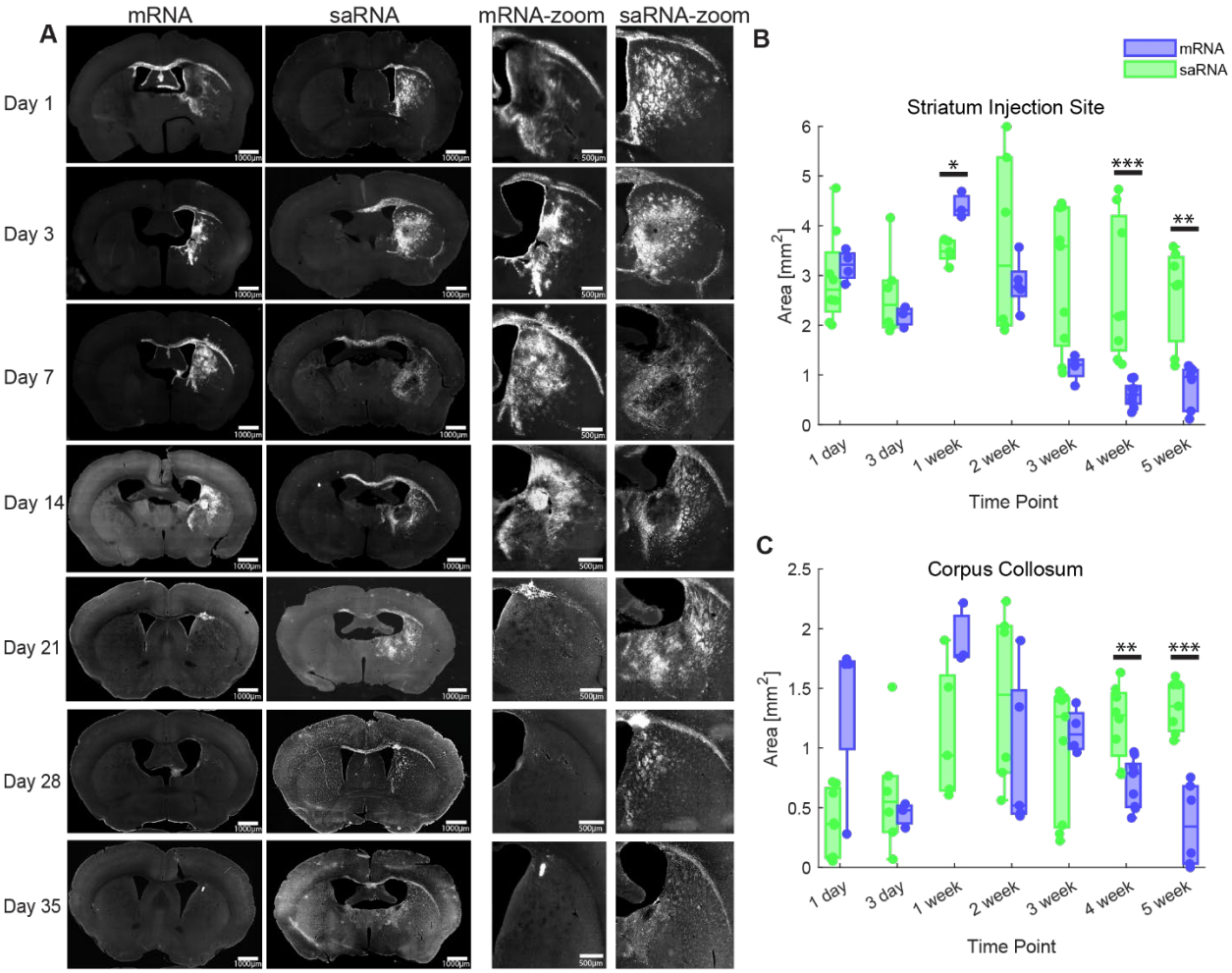

Figure 2. saRNA-LNPs mediate robust and long-lasting gene expression. (A) Example brain slices at days 1-35 post saRNA-LNP injection, showing robust mCherry fluorescence at the site of injection in the striatum. Left, whole brain slices showing injection in the right hemispheres for mRNA-LNPs and saRNA-LNPs. Right, corresponding zoomed-in views. **(B, C)** mCherry+ area around the injection site (**B**) and corpus callosum (**C**) across days post-injection. Shown are box plots (box: 1st and 3rd quartiles, horizontal line: median, whiskers: 1.5x interquartile range). ***, p<0.005; **, p<0.01; *, p<0.05, Wilcoxon rank-sum test (n=2-3 slices per mouse, 2-3 mice per time point).

saRNA-LNPs predominantly transduced astrocytes at the site of injection.

To further analyze the cell types labeled by saRNA-LNPs, we performed immunofluorescence staining using antibodies against the astrocyte marker protein GFAP or the neuronal marker protein NeuN (Fig. 3A-C). As astrocytes do not have a well-defined morphology, we calculated the fraction of mCherry positive (mCherry+) pixels that were also GFAP positive (GFAP+). We found that 43-56% of mCherry+ pixels were GFAP+ across the post injection time points examined. As neurons possess a defined morphology, we computed the fraction of mCherry+ pixels that were part of a neuron (NeuN+). Only ~1-4% of labeled pixels were neurons across the time points examined, significantly lower than astrocytes (Fig. 3D). These results demonstrate that saRNA-LNPs transfect both neurons and astrocytes, with the majority of labeled cells being astrocytes at the striatal site of injection.

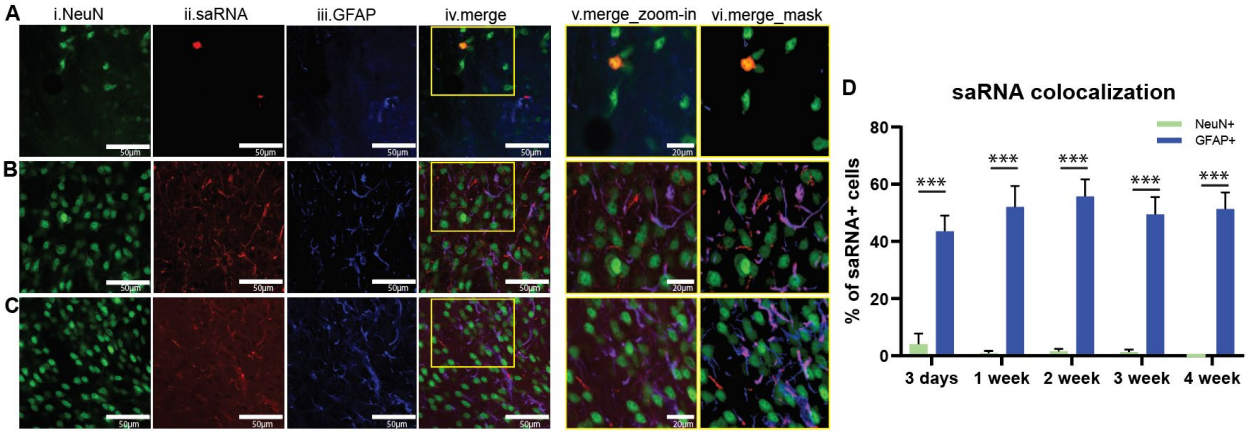

Figure 3. saRNA-LNP transfected more astrocytes than neurons in the striatum. (A) An example brain slice showing saRNA-LNP mediated gene expression in neurons. (i) NeuN immunofluorescence from neurons (green); (ii) saRNA-LNP mediated mCherry fluorescence; (iii) GFAP immunofluorescence from astrocytes (blue); (iv) Merge, showing colocalization of mCherry and NeuN immunofluorescence (orange). (v). zoomed in view of the area highlighted by yellow box in iv. (vi). Cell profiler identification of pixels positive for NeuN (green), saRNA (red), and GFAP (blue). **(B, C)** Similar to A, but for example brain slices showing saRNA-LNP mediated gene expression in astrocytes. Merge showing colocalization of mCherry and GFAP immunofluorescence (purple). **(D)** Quantification of the percentage of saRNA-mediated mCherry expression colocalization with neurons (green) versus glia (blue) across 5 time points after saRNA injection. ***, p<0.001, Wilcoxon rank-sum test (n=10-19 fields of view per timepoint).

saRNA mediates potent retrograde labeling of cortical neurons projecting to the striatal injection site

In addition to robust expression at the site of injection, we noticed that mCherry+ neurons were prominent in the cortex starting about two weeks post injection (Fig 4A-C). Many labeled neurons exhibited bright mCherry fluorescence throughout the cell bodies, and the proximal and distal processes (Fig 4C), suggesting that saRNA-LNPs retrogradely label cortical neurons projecting to the striatal injection site.

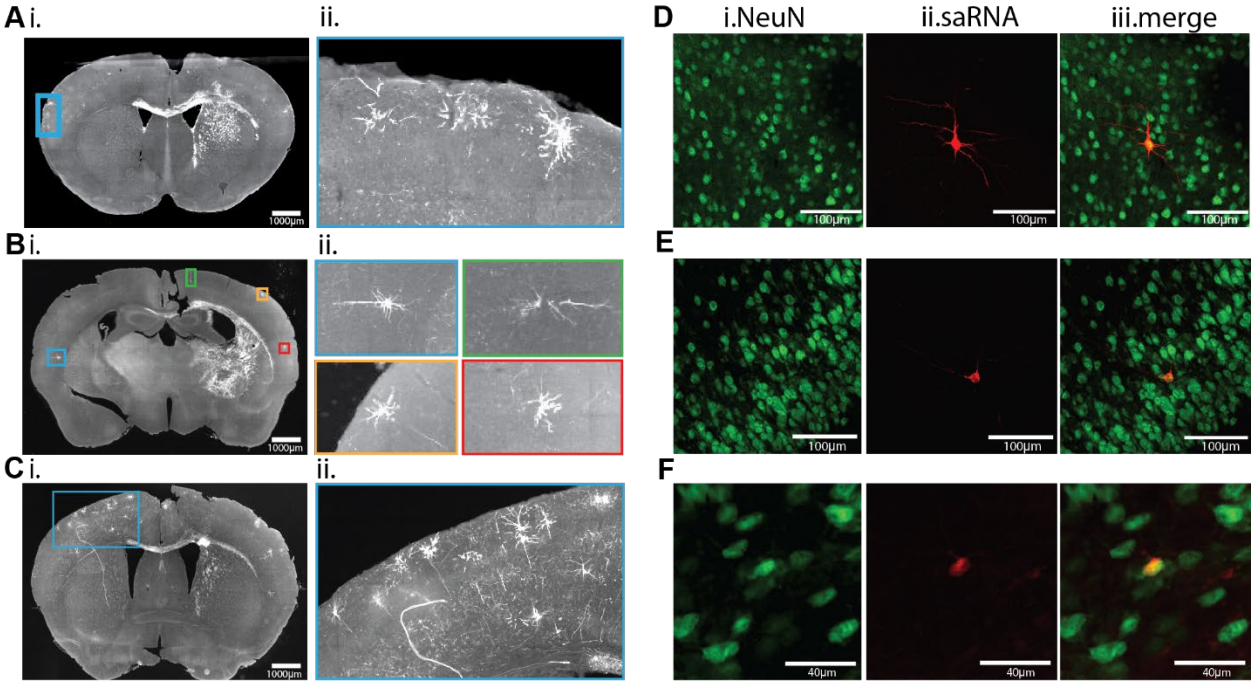

Figure 4. saRNA-LNPs retrogradely label cortical neurons. (A)(i) An example brain slice at 2 weeks post injection. (ii) A zoomed-in view of labeled cortical neurons highlighted by the blue box in A. **(B)** An example brain slice at 3 weeks post injection. (ii) Zoomed-in views of labeled cortical neurons across different areas of the cortex highlighted in blue, green, yellow, and red boxes in B. **(C)**(i) An example brain slice at 4 weeks post injection. (ii) Zoomed-in view of labeled cortical neurons highlighted by blue box in C. **(D-F)** Example fields of view showing saRNA-LNP mediated gene expression in cortical neurons. (i) NeuN immunofluorescence from neurons (green); (ii) saRNA-LNP mediated mCherry fluorescence (red); (iii) Merge, showing colocalization of mCherry and NeuN immunofluorescence (yellow).

DISCUSSION

Motivated by the exciting progress in the durable expression previously observed from modified saRNA-based vaccine technology, we examined the transfection efficiency of modified saRNA encapsulated in LNPs following intracerebral delivery in the mammalian brain. Our results show that saRNA-LNPs potently transfect brain cells at the injection site in the striatum region, and across broad cortical areas that project to the striatal injection site. hm5C saRNA-LNPs afford robust and prolonged mCherry transcript expression beyond five weeks, with some neurons remaining mCherry positive at three months post-delivery, the longest time-point examined. hm5C saRNA yields significantly longer lasting protein expression than conventional modified mRNAs.

Intriguingly, while hm5C saRNA-LNPs predominantly label astrocytes at the site of injection, many cortical neurons are also retrogradely labeled.

We tested four leading LNP formulations, identified in previous work, that exhibit excellent transfection efficiency in human and mouse cell lines. Formulations of SM102 (Spikevax®, Moderna) and ALC-0315 (Comirnaty®, BioNTech/Pfizer) effectively transfect muscle cells when formulated as vaccines. However, their transfection efficiency in the brain varies drastically, with SM102 transfecting a few cells, whereas ALC-0315 is the most potent, highlighting the distinct tissue tropism of different LNP formulations.

Recent advances in designing ionizable LNPs yield efficient mRNA delivery, particularly in vaccine development, offer promising potential for optimizing LNP-based non-viral gene transduction strategies for other tissues including the brain[1, 6, 30-33]. For example, optimizing LNP formulations improves mRNA delivery to the brain upon intrathecal [15] or intracerebroventricular injection[14], and to enhance blood brain barrier crossing[34, 35]. LNPs with improved biocompatibility enable repeated delivery of genetic payloads[30, 33]. Furthermore, LNPs can be rationally engineered to facilitate blood brain barrier crossing[35-37] and to enhance tissue and cell specificity[38]. In addition to LNPs, exosomes loaded with mRNAs encoding catalase reduce neurotoxicity and neuroinflammation in Parkinson's disease mouse models[16]. Aside from engineering LNPs, incorporating 3'UTR gene regulatory elements in saRNAs biases gene expression between astrocytes and neurons[39]. Continued efforts on engineering LNP formulations and saRNA designs will further improve transfection efficiency, cell type specific targeting, and brain specific targeting.

Our data demonstrates that modified hm5C saRNA robustly expresses mCherry protein for over five weeks after a single injection in the striatum, with mCherry fluorescence remaining prominent in some neurons even at three months post injection. This is well beyond the expression mediated by mRNA previously tested[11-16], or the seven days reported in a previous study using wild-type saRNA[17]. Importantly, we directly measured mCherry expression via microscopy. This is in sharp contrast to previous studies that reported Cre-mediated recombination process triggered by mRNA-mediated expression of Cre transcripts[14, 15, 32], which amplifies the transient presence of Cre into a more permeant recombination readout and thus cannot characterize the time course or the actual amount of mRNA transcripts.

At the striatal injection site, the hm5C saRNA-LNPs predominantly label astrocytes and a few neurons. The robust astrocyte labeling is generally in agreement with the study by Tuma et al., which showed that intracerebral injection of mRNA encoding Cre led to robust recombination-mediated astrocyte labeling in the striatum[32]. However, they observed similar labeling of astrocytes and neurons in the striatum, in contrast to the low expression observed in striatal neurons we find. As the Cre-dependent recombination assay captures transient Cre-enzyme expression, the discrepancy in transgene expression observed may reflect the time course or the magnitude variations between our study and Tuma *et al*. Indeed, the retrograding labeling of cortical neurons appears to progressively become stronger over the first couple weeks, suggesting that saRNA transcripts may accumulate slower in neurons than in astrocytes, leading to the observed low protein expression at the site of injection. However, it is also possible that ALC-0315 LNPs exhibit a low transfection rate for the medium spiny neurons that dominate the striatal neuron population. Lastly, similar to the low microglial labeling reported previously[32, 40], we

only detected a very limited instance of mCherry positive microglia labeled by our hm5C saRNA-LNPs (Supp. Fig. 2). It is surprising to detect robust retrograde labeling of cortical neurons that project to the striatum injection sites, including contralateral to the injection site. Such retrograde labeling may explain the prominent expression of mCherry observed in the corpus callosum, though it is possible that myelin may be the dominant source of the corpus callosum labeling. Future studies are needed to determine the source of mCherry fluorescence detected in the corpus callosum.

hm5C saRNA's ability to mediate long-term gene expression in brain cells presents profound therapeutic potentials, e.g., to deliver glial derived neurotrophic factors for Parkinson's disease[41], brain-derived neurotrophic factor for Alzheimer's disease[39], Bcl-2 for ischemic stroke[2, 42], apoptosis-inducing ligand for glioblastoma[43], and thrombomodulin to boost blood brain barrier integrity[44]. Additionally, continued progress to improve nonviral delivery of antisense RNA, siRNA, or CRISPR-Cas9 gene editing components into the brain will advance the ability to reduce risk factors of many neurological and psychiatric disorders[1], e.g., beta-secretase 1 or amyloid beta for Alzheimer's disease[45-48], alpha-synuclein for Parkinson's disease[49, 50], SOD1 for Amyotrophic lateral sclerosis[51], or as an immunotherapy for glioblastoma[52, 53]. Thus, hm5C saRNA-LNP represents a potent non-viral gene transduction platform for the mammalian brain with broad applicability in basic neuroscience research and exciting translational potential.

METHODS

saRNA & mRNA LNP synthesis

Both saRNA and mRNA encoding mCherry or EGFP were synthesized by *in vitro* transcription with the T7 High Yield kit (New England Biolabs). For the saRNA constructs, cytidine was replaced by 5-hydroxymethyl (TriLink). For the mRNA constructs, uridine was replaced by N1-methylpseudouridine. Following transcription for 3 hours at 37 °C, the DNA templates were digested by TurboDNase (Invitrogen). The RNA preparations were purified using the Monarch RNA KPurification kit (New England Biolabs) and eluted in water. Additionally, cellulose purification was performed as previously described to remove double-stranded RNA contaminants.[54]

The hm5C saRNA and N1mΨ mRNA encoding mCherry or EGFP were encapsulated into LNP formulations using ionizable lipids including ALC-0315 (Avanti), SM102 (Cayman), Lipid A9 (Cayman), or L319 (Cayman), in combination with DOPE (Avanti, 850725), Cholesterol (Avanti, 700100), and DMG-PEG2K (Avanti, 880151) at molar ratios of 50:38.5:10:1.5. RNA was incorporated at an N:P ratio of 10. Following encapsulation, the LNPs were dialyzed in sterile 1X Phosphate-buffered saline (PBS) overnight at 4°C. Particle size was determined via dynamic light scattering using a NanoBrook Omni (Brookhaven Instruments). Encapsulation efficiency and RNA concentration were measured with the Quantifluor RNA System (Promega). The LNPs were then concentrated with a 3 kDa MWCO Amicon Ultra Centrifugal filter to approximately 200 ng/μL and further diluted to 125ng/μL with sterile PBS. LNPs were either stored at 4˚C and administered within 3 days of preparation or stored at -20˚C until use.

Animal experiment

All animal procedures were approved by the Boston University Institutional Animal Care and Use Committee (IACUC). Male and female adult C57BL/6 mice (Jackson Labs or Charles River Laboratory) were used, and their ages were 2-5 months at the start of the experiment. During aseptic stereotaxic surgery, mice were anesthetized with isoflurane (5% for induction, 2% or less for maintenance) and preoperatively injected with sustained release buprenorphine (Ethiqa XR). LNPs loaded with saRNA or mRNA (625 ng total, 5μL at 125 ng/μL) were infused into the striatum through a small craniotomy at 3 depths (ML: -1.8mm, AP: +0.5mm, and 2μL at -2.8mm, 2μL at -2.5mm, and 1μL at -2.2mm), at a rate of 100-250 nL/min via a 10μL syringe (Hamilton Company). At the completion of all 3 infusions, the Hamilton syringe was kept in place for an additional 10 minutes before being retracted. Vetbond tissue adhesive (3M Inc) was then applied to close the incision.

Histology and immunostaining

Mice were transcardially perfused with PBS followed by 4% paraformaldehyde (PFA) buffered in PBS. Brains were collected, post-fixed in 4% PFA-PBS overnight at 4℃, and transferred to a solution with 30% sucrose in PBS at 4℃ until sinking. Brains were then sliced coronally at 50μm thickness using a freezing microtome (Leica, SM2010R) or cryostat (Leica, CM3050S). To assess the efficiency and the time course of saRNA-LNP mediated gene expression, we performed whole-slice imaging using an Olympus VS120 slide scanner microscope at 20X magnification to visualize mCherry fluorescence.

To quantify neuronal versus astrocyte targeting, we selected 2-3 sections positive for mCherry from each mouse at each desired time point using a fluorescence microscope (Leica, DFC365 FX). The selected tissue sections were then incubated in sodium citrate buffer (10mM, 6.0 pH; Sigma Aldrich, W302600) at 37℃ for 1 hour, and then transferred into a blocking solution (5% goat serum and 0.5% TritonX-100 in PBS) to prevent non-specific protein binding for 1 hour. Sections were then incubated with primary antibodies against neuronal nuclei, NeuN (rabbit, 1:500; Abcam, ab177487) and glial fibrillary acidic protein, GFAP (chicken, 1:1000; Novus Biologicals, NBP1-05198) at 4℃ overnight followed by secondary antibodies Alexafluor 488 goat anti-rabbit (1:500; Invitrogen, A11008) and Alexafluor 647 goat anti-chicken (1:500; Invitrogen, A21449) for 2 hours at room temperature. Slices were then mounted using Vectashield antifade mounting medium with DAPI (Vector Laboratories, H-1200). Immunofluorescence was then acquired using an Olympus FV3000 confocal microscope at 40X magnification and 2x zoom.

Image analysis

Colocalization analysis was performed using open-source software *CellProfiler (https://cellprofiler.org/)*. Specifically, TIFF images were loaded in CellProfiler as single-channel grayscale images, which were manually thresholded to generate masks corresponding to NeuN

positive neurons, GFAP+ glia, or mCherry+ positive objects. As neurons have defined morphology, we applied an additional filter that was optimized by manually adjusting the object area and formfactors to capture the standard shapes of neurons across all NeuN+ neurons. False positive pixels were defined as those positive for more than one marker (NeuN, GFAP, or mCherry). False positive pixels were removed from all subsequent calculations. To compute the labeling specificity of saRNA in astrocytes, we computed the ratio of pixels positive for both mCherry and GFAP over pixels positive for mCherry. To compute the labeling specificity of saRNA neurons, we computed the ratio of pixels positive for both mCherry and NeuN over the pixels positive for mCherry.

To estimate the area of RNA-mediated mCherry expression, we first manually identified the slice with the highest mCherry fluorescence in each mouse, then selected two adjacent slices. Two experimenters, blind to experimental conditions, independently segmented the areas positive for mCherry in MATLAB. As the segment areas in each slice were largely identical between the two experimenters, the mean area segmented by the two experiments was used for each slice.

Statistical analysis

Mann-Whitney Ranksum tests were used to compare the area labeled between saRNA-LNPs and mRNA-LNPs (Fig. 2), and the ratio of neuron and astrocyte labeled (Fig. 3).

ACKNOWLEDGEMENTS

X. H. acknowledges funding from NIH 1RF1NS129520, 1R01NS115797, and NSF 2002971-DIOS. M.W.G. acknowledges funding from National Science Foundation TRAILBLAZER; EFMA-2421692, Boston University Kilachand Fund, and William Fairfield Warren Professorship at Boston University. W.W.W. acknowledges funding from the Boston University Kilachand Fund. D.C.S. acknowledges funding from the American Epilepsy Society Predoctoral Fellowship. J.F. acknowledges funding from NIH T32-NS136080. E.S. acknowledges funding from NIH T32-GM008764 and NIH F31 NS143166-01. J.E.M. acknowledges funding from the NSF Graduate Research Fellowship Program 2234657 and NIH T32 Translational Research in Biomaterials Training Program (T32EB006359). This work was additionally supported by Boston University Micro and Nano Imaging Facility through NIH S10OD024993.

DATA AVAILABILITY

The data that supports the findings of this study are available upon request.

AUTHOR CONTRIBUTION

Conceptualization: WW, MWG, XH

Major data collection & analysis: JF, JEM

Support for data collection and analysis: DS, YZ, YW, CP, LD, ESA, ZY, KL, XH

Writing – Original Draft: JF, JEM, WW, MWG, XH

Writing – Review & Editing: All authors

Supervision: WW, MWG, XH

CONFLICT OF INTEREST

JEM, WW, and MWG hold an equity position in Keylicon Biosciences, a start-up that has licensed the modified saRNA technology from Boston University.

Supplemental Figures

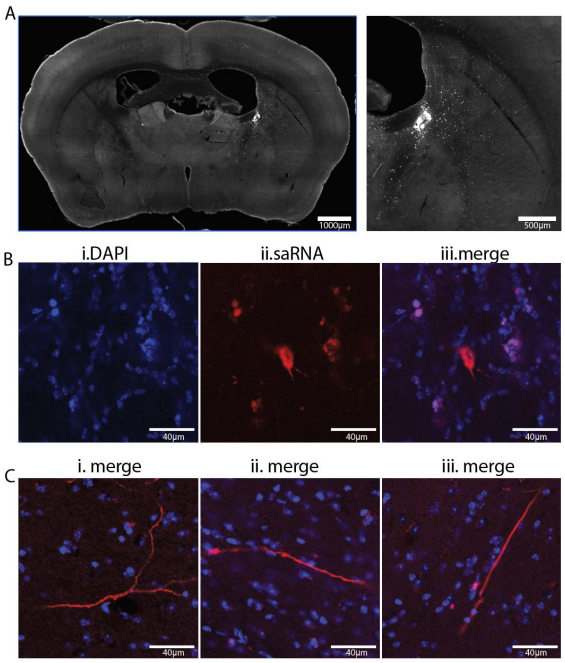

Supplemental Figure 1. saRNA-LNP demonstrates robust mCherry expression in some neurons at 3 months post injection. (A) Left; An example brain slice showing saRNA-LNP mediated mCherry expression at 3 months post-injection. Right; A zoom-in view around the injection site. **(B)** saRNA-LNP labeled cell bodies. (i) DAPI fluorescence (blue) indicating cell nuclei; (ii) saRNA-LNP mediated mCherry fluorescence; (iii) merge. (**C**) saRNA-LNP labeled neuronal processes. Shown are three example neurites (red, mCherry fluorescence), co-stained with DAPI fluorescence (blue).

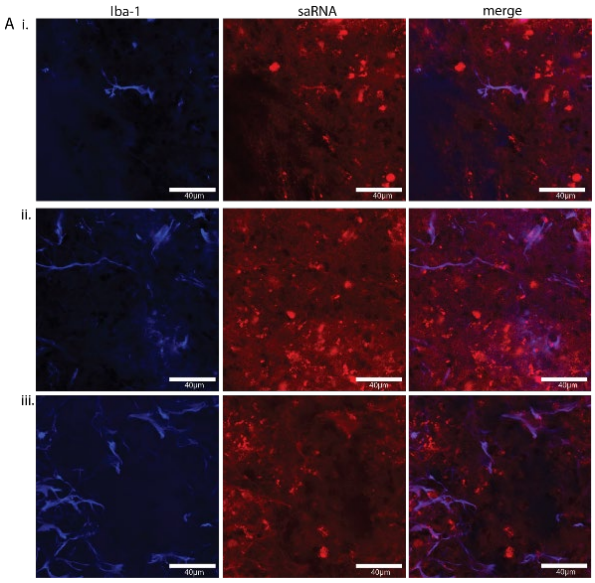

Supplemental Figure 2. saRNA-LNP mediated mCherry expression in microglia. (Ai-iii) 3 example fields of view at 1-week post injection. Left, Iba-1 immunofluorescence (blue); middle, saRNA mediated mCherry expression (red), right, merge.

References

1. Gao J, Gunasekar S, Xia ZJ, Shalin K, Jiang C, Chen H, Lee D, Lee S, Pisal ND, Luo JN, Griciuc A, Karp JM, Tanzi R, Joshi N. Gene therapy for CNS disorders: modalities, delivery and translational challenges. Nat Rev Neurosci. 2024;25(8):553–72. Epub 20240619. doi: 10.1038/s41583-024-00829-7. PubMed PMID: 38898231.
2. Toyoda K, Chu Y, Heistad DD. Gene therapy for cerebral vascular disease: update 2003. Br J Pharmacol. 2003;139(1):1–9. doi: 10.1038/sj.bjp.0705217. PubMed PMID: 12746217; PMCID: PMC1573819.
3. Han X. Optogenetics in the nonhuman primate. Prog Brain Res. 2012;196:215–33. Epub 2012/02/22. doi: 10.1016/B978-0-444-59426-6.00011-2. PubMed PMID: 22341328.
4. Han X. In vivo application of optogenetics for neural circuit analysis. ACS Chem Neurosci. 2012;3(8):577–84. Epub 2012/08/17. doi: 10.1021/cn300065j. PubMed PMID: 22896801; PMCID: 3419447.
5. Anthony K. RNA-based therapeutics for neurological diseases. RNA Biol. 2022;19(1):176–90. Epub 20211231. doi: 10.1080/15476286.2021.2021650. PubMed PMID: 35067193; PMCID: PMC8786337.
6. Khare P, Edgecomb SX, Hamadani CM, Tanner EEL, D SM. Lipid nanoparticle-mediated drug delivery to the brain. Advanced drug delivery reviews. 2023;197:114861. Epub 20230506. doi: 10.1016/j.addr.2023.114861. PubMed PMID: 37150326.
7. Kariko K, Muramatsu H, Welsh FA, Ludwig J, Kato H, Akira S, Weissman D. Incorporation of pseudouridine into mRNA yields superior nonimmunogenic vector with increased translational capacity and biological stability. Mol Ther. 2008;16(11):1833–40. Epub 20080916. doi: 10.1038/mt.2008.200. PubMed PMID: 18797453; PMCID: PMC2775451.
8. Kormann MS, Hasenpusch G, Aneja MK, Nica G, Flemmer AW, Herber-Jonat S, Huppmann M, Mays LE, Illenyi M, Schams A, Griese M, Bittmann I, Handgretinger R, Hartl D, Rosenecker J, Rudolph C. Expression of therapeutic proteins after delivery of chemically modified mRNA in mice. Nat Biotechnol. 2011;29(2):154–7. Epub 20110109. doi: 10.1038/nbt.1733. PubMed PMID: 21217696.
9. Anderson BR, Muramatsu H, Nallagatla SR, Bevilacqua PC, Sansing LH, Weissman D, Kariko K. Incorporation of pseudouridine into mRNA enhances translation by diminishing PKR activation. Nucleic acids research. 2010;38(17):5884–92. Epub 20100510. doi: 10.1093/nar/gkq347. PubMed PMID: 20457754; PMCID: PMC2943593.
10. Polack FP, Thomas SJ, Kitchin N, Absalon J, Gurtman A, Lockhart S, Perez JL, Perez Marc G, Moreira ED, Zerbini C, Bailey R, Swanson KA, Roychoudhury S, Koury K, Li P, Kalina WV, Cooper D, Frenck RW, Jr., Hammitt LL, Tureci O, Nell H, Schaefer A, Unal S, Tresnan DB, Mather S, Dormitzer PR, Sahin U, Jansen KU, Gruber WC, Group CCT. Safety and Efficacy of the BNT162b2 mRNA Covid-19 Vaccine. N Engl J Med. 2020;383(27):2603–15. Epub 20201210. doi: 10.1056/NEJMoa2034577. PubMed PMID: 33301246; PMCID: PMC7745181.
11. Kariko K, Keller JM, Harris VA, Langer DJ, Welsh FA. In vivo protein expression from mRNA delivered into adult rat brain. J Neurosci Methods. 2001;105(1):77–86. doi: 10.1016/s0165-0270(00)00355-1. PubMed PMID: 11166368.

12. Tanaka H, Nakatani T, Furihata T, Tange K, Nakai Y, Yoshioka H, Harashima H, Akita H. In Vivo Introduction of mRNA Encapsulated in Lipid Nanoparticles to Brain Neuronal Cells and Astrocytes via Intracerebroventricular Administration. Molecular pharmaceutics. 2018;15(5):2060–7. Epub 20180411. doi: 10.1021/acs.molpharmaceut.7b01084. PubMed PMID: 29638135.
13. Li Y, Jarvis R, Zhu K, Glass Z, Ogurlu R, Gao P, Li P, Chen J, Yu Y, Yang Y, Xu Q. Protein and mRNA Delivery Enabled by Cholesteryl-Based Biodegradable Lipidoid Nanoparticles. Angew Chem Int Ed Engl. 2020;59(35):14957–64. Epub 20200615. doi: 10.1002/anie.202004994. PubMed PMID: 32438474; PMCID: PMC7679290.
14. Palanki R, Bose SK, Dave A, White BM, Berkowitz C, Luks V, Yaqoob F, Han E, Swingle KL, Menon P, Hodgson E, Biswas A, Billingsley MM, Li L, Yiping F, Carpenter M, Trokhan A, Yeo J, Johana N, Wan TY, Alameh MG, Bennett FC, Storm PB, Jain R, Chan J, Weissman D, Mitchell MJ, Peranteau WH. Ionizable Lipid Nanoparticles for Therapeutic Base Editing of Congenital Brain Disease. ACS Nano. 2023;17(14):13594–610. Epub 20230717. doi: 10.1021/acsnano.3c02268. PubMed PMID: 37458484; PMCID: PMC11025390.
15. Xue Y, Wang C, Li H, Du S, Zhong Y, Zhang Y, Wang S, Guo K, Hou X, Kang DD, Liu Z, Tian M, Cao D, Deng B, McComb DW, Markovic T, Pan J, Borna M, Nestler EJ, Peng PC, Dong Y. Lipid Nanoparticles Enhance mRNA Delivery to the Central Nervous System Upon Intrathecal Injection. Adv Mater. 2025;37(27):e2417097. Epub 20250503. doi: 10.1002/adma.202417097. PubMed PMID: 40317512; PMCID: PMC12245596.
16. Kojima R, Bojar D, Rizzi G, Hamri GC, El-Baba MD, Saxena P, Auslander S, Tan KR, Fussenegger M. Designer exosomes produced by implanted cells intracerebrally deliver therapeutic cargo for Parkinson's disease treatment. Nat Commun. 2018;9(1):1305. Epub 20180403. doi: 10.1038/s41467-018-03733-8. PubMed PMID: 29610454; PMCID: PMC5880805.
17. Kim M, Oh J, Lee Y, Lee EH, Ko SH, Jeong JH, Park CH, Lee M. Delivery of self-replicating messenger RNA into the brain for the treatment of ischemic stroke. J Control Release. 2022;350:471–85. Epub 20220831. doi: 10.1016/j.jconrel.2022.08.049. PubMed PMID: 36041589.
18. Minnaert AK, Vanluchene H, Verbeke R, Lentacker I, De Smedt SC, Raemdonck K, Sanders NN, Remaut K. Strategies for controlling the innate immune activity of conventional and self-amplifying mRNA therapeutics: Getting the message across. Advanced drug delivery reviews. 2021;176:113900. Epub 20210726. doi: 10.1016/j.addr.2021.113900. PubMed PMID: 34324884; PMCID: PMC8325057.
19. Kairuz D, Samudh N, Ely A, Arbuthnot P, Bloom K. Advancing mRNA technologies for therapies and vaccines: An African context. Front Immunol. 2022;13:1018961. Epub 20221024. doi: 10.3389/fimmu.2022.1018961. PubMed PMID: 36353641; PMCID: PMC9637871.
20. Voigt EA, Gerhardt A, Hanson D, Jennewein MF, Battisti P, Reed S, Singh J, Mohamath R, Bakken J, Beaver S, Press C, Soon-Shiong P, Paddon CJ, Fox CB, Casper C. A self-amplifying RNA vaccine against COVID-19 with long-term room-temperature stability. NPJ Vaccines. 2022;7(1):136. Epub 20221102. doi: 10.1038/s41541-022-00549-y. PubMed PMID: 36323666; PMCID: PMC9628444.

21. Beissert T, Perkovic M, Vogel A, Erbar S, Walzer KC, Hempel T, Brill S, Haefner E, Becker R, Tureci O, Sahin U. A Trans-amplifying RNA Vaccine Strategy for Induction of Potent Protective Immunity. Mol Ther. 2020;28(1):119–28. Epub 20190912. doi: 10.1016/j.ymthe.2019.09.009. PubMed PMID: 31624015; PMCID: PMC6953774.
22. Erasmus JH, Archer J, Fuerte-Stone J, Khandhar AP, Voigt E, Granger B, Bombardi RG, Govero J, Tan Q, Durnell LA, Coler RN, Diamond MS, Crowe JE, Jr., Reed SG, Thackray LB, Carnahan RH, Van Hoeven N. Intramuscular Delivery of Replicon RNA Encoding ZIKV-117 Human Monoclonal Antibody Protects against Zika Virus Infection. Mol Ther Methods Clin Dev. 2020;18:402–14. Epub 20200618. doi: 10.1016/j.omtm.2020.06.011. PubMed PMID: 32695842; PMCID: PMC7363633.
23. Blakney AK, McKay PF, Christensen D, Yus BI, Aldon Y, Follmann F, Shattock RJ. Effects of cationic adjuvant formulation particle type, fluidity and immunomodulators on delivery and immunogenicity of saRNA. J Control Release. 2019;304:65–74. Epub 20190506. doi: 10.1016/j.jconrel.2019.04.043. PubMed PMID: 31071377.
24. Papukashvili D, Rcheulishvili N, Liu C, Ji Y, He Y, Wang PG. Self-Amplifying RNA Approach for Protein Replacement Therapy. International journal of molecular sciences. 2022;23(21). Epub 20221025. doi: 10.3390/ijms232112884. PubMed PMID: 36361673; PMCID: PMC9655356.
25. Kairuz D, Samudh N, Ely A, Arbuthnot P, Bloom K. Production, Characterization, and Assessment of Permanently Cationic and Ionizable Lipid Nanoparticles for Use in the Delivery of Self-Amplifying RNA Vaccines. Pharmaceutics. 2023;15(4). Epub 20230407. doi: 10.3390/pharmaceutics15041173. PubMed PMID: 37111658; PMCID: PMC10143526.
26. Deering RP, Kommareddy S, Ulmer JB, Brito LA, Geall AJ. Nucleic acid vaccines: prospects for non-viral delivery of mRNA vaccines. Expert Opin Drug Deliv. 2014;11(6):885–99. Epub 20140326. doi: 10.1517/17425247.2014.901308. PubMed PMID: 24665982.
27. Pollock KM, Cheeseman HM, Szubert AJ, Libri V, Boffito M, Owen D, Bern H, O'Hara J, McFarlane LR, Lemm NM, McKay PF, Rampling T, Yim YTN, Milinkovic A, Kingsley C, Cole T, Fagerbrink S, Aban M, Tanaka M, Mehdipour S, Robbins A, Budd W, Faust SN, Hassanin H, Cosgrove CA, Winston A, Fidler S, Dunn DT, McCormack S, Shattock RJ, Group Cs. Safety and immunogenicity of a self-amplifying RNA vaccine against COVID-19: COVAC1, a phase I, dose-ranging trial. EClinicalMedicine. 2022;44:101262. Epub 20220114. doi: 10.1016/j.eclinm.2021.101262. PubMed PMID: 35043093; PMCID: PMC8759012.
28. McGee JE, Kirsch JR, Kenney D, Cerbo F, Chavez EC, Shih TY, Douam F, Wong WW, Grinstaff MW. Complete substitution with modified nucleotides in self-amplifying RNA suppresses the interferon response and increases potency. Nat Biotechnol. 2024. Epub 20240708. doi: 10.1038/s41587-024-02306-z. PubMed PMID: 38977924; PMCID: PMC11707045.
29. Han X, Zhang H, Butowska K, Swingle KL, Alameh MG, Weissman D, Mitchell MJ. An ionizable lipid toolbox for RNA delivery. Nat Commun. 2021;12(1):7233. Epub 20211213. doi: 10.1038/s41467-021-27493-0. PubMed PMID: 34903741; PMCID: PMC8668901.
30. Hou X, Zaks T, Langer R, Dong Y. Lipid nanoparticles for mRNA delivery. Nat Rev Mater. 2021;6(12):1078–94. Epub 20210810. doi: 10.1038/s41578-021-00358-0. PubMed PMID: 34394960; PMCID: PMC8353930.

31. Luo D, Saltzman WM. Synthetic DNA delivery systems. Nat Biotechnol. 2000;18(1):33–7. Epub 2000/01/14. doi: 10.1038/71889. PubMed PMID: 10625387.
32. Tuma J, Chen YJ, Collins MG, Paul A, Li J, Han H, Sharma R, Murthy N, Lee HY. Lipid Nanoparticles Deliver mRNA to the Brain after an Intracerebral Injection. Biochemistry. 2023;62(24):3533–47. Epub 20230920. doi: 10.1021/acs.biochem.3c00371. PubMed PMID: 37729550; PMCID: PMC10760911.
33. Raguram A, Banskota S, Liu DR. Therapeutic in vivo delivery of gene editing agents. Cell. 2022;185(15):2806–27. Epub 20220706. doi: 10.1016/j.cell.2022.03.045. PubMed PMID: 35798006; PMCID: PMC9454337.
34. Byun MJ, Lim J, Kim SN, Park DH, Kim TH, Park W, Park CG. Advances in Nanoparticles for Effective Delivery of RNA Therapeutics. Biochip J. 2022;16(2):128–45. Epub 20220303. doi: 10.1007/s13206-022-00052-5. PubMed PMID: 35261724; PMCID: PMC8891745.
35. Han EL, Padilla MS, Palanki R, Kim D, Mrksich K, Li JJ, Tang S, Yoon IC, Mitchell MJ. Predictive High-Throughput Platform for Dual Screening of mRNA Lipid Nanoparticle Blood-Brain Barrier Transfection and Crossing. Nano Lett. 2024;24(5):1477–86. Epub 20240123. doi: 10.1021/acs.nanolett.3c03509. PubMed PMID: 38259198; PMCID: PMC11922166.
36. Cao D, Hou X, Wang C, Wang S, Liu Z, Tian M, Guo K, Li H, Kang DD, Zhong Y, Xue Y, Yu C, Deng B, Dong Y. Lipid nanoparticles for mRNA delivery in brain via systemic administration. Sci Adv. 2025;11(33):eadw0730. Epub 20250813. doi: 10.1126/sciadv.adw0730. PubMed PMID: 40802746; PMCID: PMC12346281.
37. Wang C, Xue Y, Markovic T, Li H, Wang S, Zhong Y, Du S, Zhang Y, Hou X, Yu Y, Liu Z, Tian M, Kang DD, Wang L, Guo K, Cao D, Yan J, Deng B, McComb DW, Parsons RE, Minier-Toribio AM, Holt LM, Pan J, Hashemi A, Kopell BH, Charney AW, Nestler EJ, Peng PC, Dong Y. Blood-brain-barrier-crossing lipid nanoparticles for mRNA delivery to the central nervous system. Nat Mater. 2025;24(10):1653–63. Epub 20250217. doi: 10.1038/s41563-024-02114-5. PubMed PMID: 39962245; PMCID: PMC12514551.
38. Kim J, Eygeris Y, Ryals RC, Jozic A, Sahay G. Strategies for non-viral vectors targeting organs beyond the liver. Nat Nanotechnol. 2024;19(4):428–47. Epub 20231227. doi: 10.1038/s41565-023-01563-4. PubMed PMID: 38151642.
39. Li H, Cao Y, Ye J, Yang Z, Chen Q, Liu X, Zhang B, Qiao J, Tang Q, Yang H, Li J, Shi Z, Mao Y. Engineering brain-derived neurotrophic factor mRNA delivery for the treatment of Alzheimer's disease. Chemical Engineering Journal. 2023;466:143152. doi: https://doi.org/10.1016/j.cej.2023.143152.
40. Sela M, Chen G, Kadosh H, Kagan T, Nicola R, Turutov S, Richtman Y, Zhige L, Albalak Menasherov MR, Kagan S, Schroeder T, Mora-Raimundo P, Kablan R, Egorov E, Odeh A, Abu-Raiya T, Ionita I, Freilich I, Kaneti G, Knani I, Arav Y, Leichtmann-Bardoogo Y, Tadmor K, Shklover J, Patriarchi T, Danino D, Hasson P, Ashery U, Zeisel A, Maoz BM, Laviv T, Radinsky K, Schroeder A. AI-Validated Brain Targeted mRNA Lipid Nanoparticles with Neuronal Tropism. ACS Nano. 2025;19(41):36106–28. Epub 20250916. doi: 10.1021/acsnano.4c15013. PubMed PMID: 40957853.
41. Bleier BS, Kohman RE, Guerra K, Nocera AL, Ramanlal S, Kocharyan AH, Curry WT, Han X. Heterotopic Mucosal Grafting Enables the Delivery of Therapeutic Neuropeptides

Across the Blood Brain Barrier. Neurosurgery. 2016;78(3):448–57; discussion 57. Epub 2015/09/10. doi: 10.1227/NEU.0000000000001016. PubMed PMID: 26352099.
42. Lawrence MS, McLaughlin JR, Sun GH, Ho DY, McIntosh L, Kunis DM, Sapolsky RM, Steinberg GK. Herpes simplex viral vectors expressing Bcl-2 are neuroprotective when delivered after a stroke. J Cereb Blood Flow Metab. 1997;17(7):740–4. doi: 10.1097/00004647-199707000-00003. PubMed PMID: 9270490.
43. Peng H, Guo X, He J, Duan C, Yang M, Zhang X, Zhang L, Fu R, Wang B, Wang D, Chen H, Xie M, Feng P, Dai L, Tang X, Luo J. Intracranial delivery of synthetic mRNA to suppress glioblastoma. Mol Ther Oncolytics. 2022;24:160–70. Epub 20211214. doi: 10.1016/j.omto.2021.12.010. PubMed PMID: 35024442; PMCID: PMC8724946.
44. Marcos-Contreras OA, Greineder CF, Kiseleva RY, Parhiz H, Walsh LR, Zuluaga-Ramirez V, Myerson JW, Hood ED, Villa CH, Tombacz I, Pardi N, Seliga A, Mui BL, Tam YK, Glassman PM, Shuvaev VV, Nong J, Brenner JS, Khoshnejad M, Madden T, Weissmann D, Persidsky Y, Muzykantov VR. Selective targeting of nanomedicine to inflamed cerebral vasculature to enhance the blood-brain barrier. Proc Natl Acad Sci U S A. 2020;117(7):3405–14. Epub 20200131. doi: 10.1073/pnas.1912012117. PubMed PMID: 32005712; PMCID: PMC7035611.
45. Shyam R, Ren Y, Lee J, Braunstein KE, Mao HQ, Wong PC. Intraventricular Delivery of siRNA Nanoparticles to the Central Nervous System. Mol Ther Nucleic Acids. 2015;4:e242. Epub 20150512. doi: 10.1038/mtna.2015.15. PubMed PMID: 25965552.
46. Yang X, Yang W, Xia X, Lei T, Yang Z, Jia W, Zhou Y, Cheng G, Gao H. Intranasal Delivery of BACE1 siRNA and Rapamycin by Dual Targets Modified Nanoparticles for Alzheimer's Disease Therapy. Small. 2022;18(30):e2203182. Epub 20220630. doi: 10.1002/smll.202203182. PubMed PMID: 35771092.
47. Wang P, Zheng X, Guo Q, Yang P, Pang X, Qian K, Lu W, Zhang Q, Jiang X. Systemic delivery of BACE1 siRNA through neuron-targeted nanocomplexes for treatment of Alzheimer's disease. J Control Release. 2018;279:220–33. Epub 20180419. doi: 10.1016/j.jconrel.2018.04.034. PubMed PMID: 29679667.
48. Zhou Y, Zhu F, Liu Y, Zheng M, Wang Y, Zhang D, Anraku Y, Zou Y, Li J, Wu H, Pang X, Tao W, Shimoni O, Bush AI, Xue X, Shi B. Blood-brain barrier-penetrating siRNA nanomedicine for Alzheimer's disease therapy. Sci Adv. 2020;6(41). Epub 20201009. doi: 10.1126/sciadv.abc7031. PubMed PMID: 33036977; PMCID: PMC7546706.
49. Helmschrodt C, Hobel S, Schoniger S, Bauer A, Bonicelli J, Gringmuth M, Fietz SA, Aigner A, Richter A, Richter F. Polyethylenimine Nanoparticle-Mediated siRNA Delivery to Reduce alpha-Synuclein Expression in a Model of Parkinson's Disease. Mol Ther Nucleic Acids. 2017;9:57–68. Epub 20170830. doi: 10.1016/j.omtn.2017.08.013. PubMed PMID: 29246324; PMCID: PMC5602522.
50. Schlich M, Longhena F, Faustini G, O'Driscoll CM, Sinico C, Fadda AM, Bellucci A, Lai F. Anionic liposomes for small interfering ribonucleic acid (siRNA) delivery to primary neuronal cells: Evaluation of alpha-synuclein knockdown efficacy. Nano Research. 2017;10(10):3496–508. doi: 10.1007/s12274-017-1561-z.
51. Xie Q, Li K, Chen Y, Li Y, Jiang W, Cao W, Yu H, Fan D, Deng B. Gene therapy breakthroughs in ALS: a beacon of hope for 20% of ALS patients. Transl Neurodegener.

2025;14(1):19. Epub 20250416. doi: 10.1186/s40035-025-00477-6. PubMed PMID: 40234983; PMCID: PMC12001736.
52. Liu S, Liu J, Li H, Mao K, Wang H, Meng X, Wang J, Wu C, Chen H, Wang X, Cong X, Hou Y, Wang Y, Wang M, Yang YG, Sun T. An optimized ionizable cationic lipid for brain tumor-targeted siRNA delivery and glioblastoma immunotherapy. Biomaterials. 2022;287:121645. Epub 20220622. doi: 10.1016/j.biomaterials.2022.121645. PubMed PMID: 35779480.
53. Rosenblum D, Gutkin A, Kedmi R, Ramishetti S, Veiga N, Jacobi AM, Schubert MS, Friedmann-Morvinski D, Cohen ZR, Behlke MA, Lieberman J, Peer D. CRISPR-Cas9 genome editing using targeted lipid nanoparticles for cancer therapy. Sci Adv. 2020;6(47). Epub 20201118. doi: 10.1126/sciadv.abc9450. PubMed PMID: 33208369; PMCID: PMC7673804.
54. Baiersdorfer M, Boros G, Muramatsu H, Mahiny A, Vlatkovic I, Sahin U, Kariko K. A Facile Method for the Removal of dsRNA Contaminant from In Vitro-Transcribed mRNA. Mol Ther Nucleic Acids. 2019;15:26–35. Epub 20190227. doi: 10.1016/j.omtn.2019.02.018. PubMed PMID: 30933724; PMCID: PMC6444222.